Femtosecond Coulomb Explosion Imaging of Vibrational Wave Functions

S. Chelkowski,[1] P. B. Corkum,[2] and A. D. Bandrauk[1]
[1]*Université de Sherbrooke, Sherbrooke, Quebec, Canada J1K 2R1*
[2]*National Research Council of Canada, Ottawa, Ontario, Canada K1A 0R6*
(Received 5 October 1998)

Because of the nonlinearity of multiphoton ionization, an intense 5 fs pulse is short enough to change the ionization probability from near zero to near unity in less than one-half of a laser period. For H_2^+ this exposes all parts of the vibrational wave function to the full force of Coulomb repulsion at nearly the same time. By solving the time dependent Schrödinger equation, following both electron and ion motion we show that the initial vibrational wave function $\Psi(R)$ of H_2^+ can be reconstructed by using Coulomb's law to map the ion fragment kinetic energy spectrum into $|\Psi(R)|^2$. [S0031-9007(99)08986-3]

PACS numbers: 33.80.Rv, 34.50.Gb

Molecular structure and its transformations during reactions play a large role in our understanding of chemistry. Molecular spectroscopy has been the primary tool used to determine the geometry of small equilibrium molecules. Dynamics introduces a new complexity since the structure now changes. Following changing structure spectroscopically is a major challenge. However, spectroscopy remains the only approach that is technically feasible today. Thus, femtosecond experiments have concentrated on applying two (or more)-photon spectroscopy in the time domain. (i) A molecule is excited from the ground state to a state on which dynamics is to be observed; (ii) the evolution is followed by using a second pulse to project the evolving wave packet onto a third (reference) state. The problem is that if the intermediate surface is unknown, then the reference surface is probably also unknown. The inversion problem is very complex in a molecule with no fixed structure and a poorly known reference state.

Coulomb explosion imaging, electron beam, and x-ray scattering are all alternatives to spectroscopy for determining equilibrium structure. The technology is only now being developed that could allow these methods to determine changing structure during dynamics. By simulating optical Coulomb explosion imaging [1–4] we show a path to directly imaging structural changes during dynamics of small molecules. We concentrate on H_2^+, where a full electron-nuclear non-Born-Oppenheimer calculation, valid even for strong laser fields, has now been achieved [5]. The subsequent Coulomb explosion produces protons with kinetic energy determined by the initial conditions and by Coulomb's law. We investigate the accuracy of the classical Coulomb explosion approximation, isolate the inherently quantum mechanical features of the image reconstruction, and show images can be accurately obtained.

This paper should be viewed in the context of Coulomb explosion imaging that uses ion-foil collisions [6]. In those experiments, MeV molecular ions pass through a thin (<100 Å) gold foil where they lose many electrons. The transit time through the foil is between 0.1 and 1 fs. When the ions emerge from the foil they repel each other (explode) and the explosion pattern is used to determine the original molecular geometry.

Optical Coulomb explosion imaging replaces the molecule-foil collision with multiphoton ionization. The technical advance that has motivated these calculations has been the development of high power laser pulses with a duration of only a few femtoseconds [7] in the 800 nm region. We show that multiphoton ionization rates can rise so rapidly [8–10] with laser intensity that the ionization probability can go from ~0 to ~1 in less than one-half an optical period (~1 fs). Once released, an electron in a strong optical field is removed from the molecule's vicinity in a small fraction of an optical period [11]. Thus, we demonstrate that intense ultrashort laser pulses allow measurements with resolution determined by the oscillation period of the light rather than the duration of the pulse envelope.

Specifically, we solve the three-body, time dependent Schrödinger equation for the H_2^+ molecule in a strong laser field (in one dimension):

$$i\,\frac{\partial\psi(R,z,t)}{\partial t} = H(R,z,t)\psi(R,z,t)\,, \qquad (1)$$

where R is the internuclear distance, z is the electron position with respect to the two protons center of mass and $H(R,z,t)$ is the three-body Hamiltonian [5]. (Atomic units are used throughout the paper.) We assume that H_2^+ is prepared in a specific vibrational state (we used $v = 2$ or $v = 6$)

$$\psi(R,z,0) = \psi_{\rm in}(R)\psi_e(R,z)\,, \qquad (2)$$

where $\Psi_e(R,z)$ is the Σ_g eigenfunction of the electronic part in the Hamiltonian H and $\Psi_{\rm in}(R)$ is the initial vibrational wave function. We use experimentally realistic pulses with a slightly modified (for numerical convenience) Gaussian intensity profile, solving Eq. (1) to find the wave function $\Psi(R,z,t_{\rm final})$ where $t_{\rm final} = 43$ fs. By then the molecule is completely ionized and the nuclear wave packet is at $R > 18$ au. At $t_{\rm final}$ we project $\Psi(R,z,t)$ onto asymptotic (large R, $l = 0$) Coulomb

 0031-9007/99/82(17)/3416(4)$15.00

radial functions [12] getting $\Psi(p, z, t_{\text{final}})$, where p is the asymptotic momentum. Then the kinetic energy spectrum $S(E)$ is calculated as the integral over z of $|\Psi(p, z, t_{\text{final}})|^2 m/p$, where E is the total energy of protons in their center of mass system.

In general there is no simple mapping between $S(E)$ and the initial vibrational wave function [they are related by the integral equation, Eq. (4)]. However, assuming a classical explosion occurs with an R-dependent probability distribution $|\psi_{\text{CEI}}(R)|^2$ with initial zero kinetic energy, we obtain a simple relation between this distribution and $S(E)$ by using energy conservation. Thus after equating the distribution in R and E spaces: $S(E)dE = |\psi_{\text{CEI}}(R)|^2 dR$ we get

$$|\psi_{\text{CEI}}(R)|^2 = |S(E)| \frac{q^2}{R^2}, \tag{3}$$

where the factor q^2/R^2 is a Jacobian $|dE/dR|$.

The pulse intensity appropriate for Coulomb explosion imaging is determined by calculating the ionization probability following a $\frac{1}{2}$-period duration sine wave pulse shown in the inset in Fig. 1. The ionization probability approaches unity at 4×10^{15} W/cm^2, independent of the separation of the protons. We propose to pass 10^{15} W/cm^2, where ionization rates are $\sim 10^{15}$ sec^{-1}, as the intensity changes most rapidly. Then, if the pulse is short enough, the ionization probability changes from near zero to near one in less than $\frac{1}{2}$ of a period ($\sim$1 fs). Consequently, for the remainder of the calculation, we use a peak pulse intensity of 4×10^{15} W/cm^2.

Figure 2 shows the initial $|\Psi_{\text{in}}(R)|^2$ for H_2^+ and the Coulomb explosion imaged $|\Psi_{\text{CEI}}(R)|^2$ (solid curve) achieved in our simulations for a $\tau_p = 4.5$ fs (full width at half maximum) pulse with a peak intensity of 4×10^{15} W/cm^2 (see Fig. 2, inset). Such pulse characteristics are similar to those used in recent experiments on high-harmonic generation [13].

For many dynamics applications being able to obtain an image of the quality of $|\Psi_{\text{CEI}}(R)|^2$ would be a major advance. However, the zeros of the wave function are not completely achieved in $|\Psi_{\text{CEI}}(R)|^2$, there is a small shift to larger R's, and there is an error in the amplitude. If future dynamics experiments are to rely on Coulomb explosion imaging, it is important to investigate the origin of these anomalies (Figs. 3 and 4).

Figures 3(a) and 3(b) show results for imaging both the $v = 2$ and $v = 6$ vibrational states ionized with a 3.2 fs, 800 nm pulse [shown in the inset in Fig. 3(a)]. ($v = 6$ was chosen to make the classical energy of the molecular vibration easily observable on top of the Coulomb explosion energy, allowing us to observe the influence of the initial momentum distribution.) Compared with Fig. 2, the calculated Coulomb explosion imaged data in Fig. 3(a) is a more faithful reproduction of the original wave function. The difference between Figs. 2 and 3(a) is caused by motion on the laser-modified potential curves [9,14] of H_2^+ before ionization occurs. A small further improvement is seen with 1.7 fs, 212 nm pulses (not shown). (Although motion on the laser-modified curves is observable in H_2^+ imaging with currently available 4.5 fs laser pulses, it will be negligible for higher mass atoms.)

To study anomalies in the amplitude of the reconstructed wave function, we instantly place an initial vibrational wave function on the Coulomb repulsive surface. This procedure simulates Coulomb explosion imaging (it corresponds to instantaneous, 100% ionization) without the complexity of the strong laser field and the accompanying electronic transitions. It allows us to clearly identify the underlying physical phenomena.

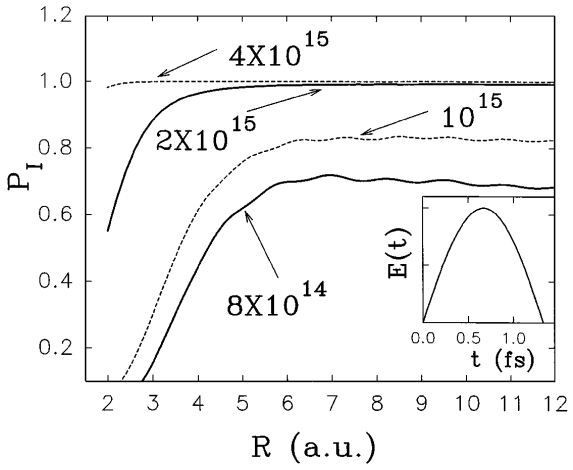

FIG. 1. Ionization probability for H_2^+ in one-half period of 800 nm light plotted as a function of the internuclear separation for different peak laser fields. The fields are labeled by their corresponding laser intensity in W/cm^2. The time dependent field of the $\frac{1}{2}$-period sine wave pulse is shown in the insert.

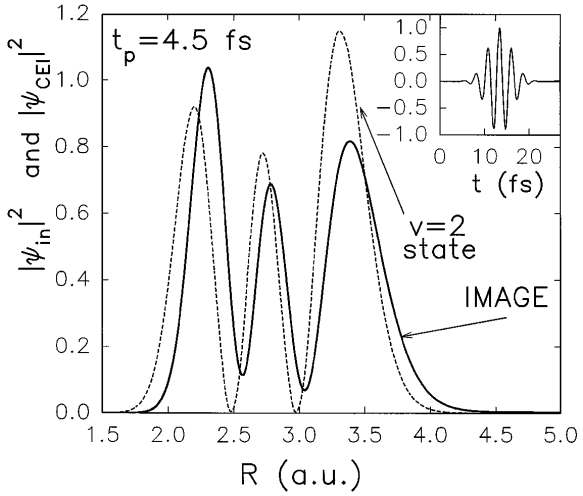

FIG. 2. $|\Psi_{\text{in}}(R)|^2$ for the $v = 2$ vibrational state of H_2^+ plotted together with the simulated Coulomb explosion imaged $|\Psi_{\text{CEI}}(R)|^2$. For this calculation the peak laser intensity was 4×10^{15} W/cm^2 and the time dependent electric field for the 4.5 fs full width at half maximum pulse is shown in the inset.

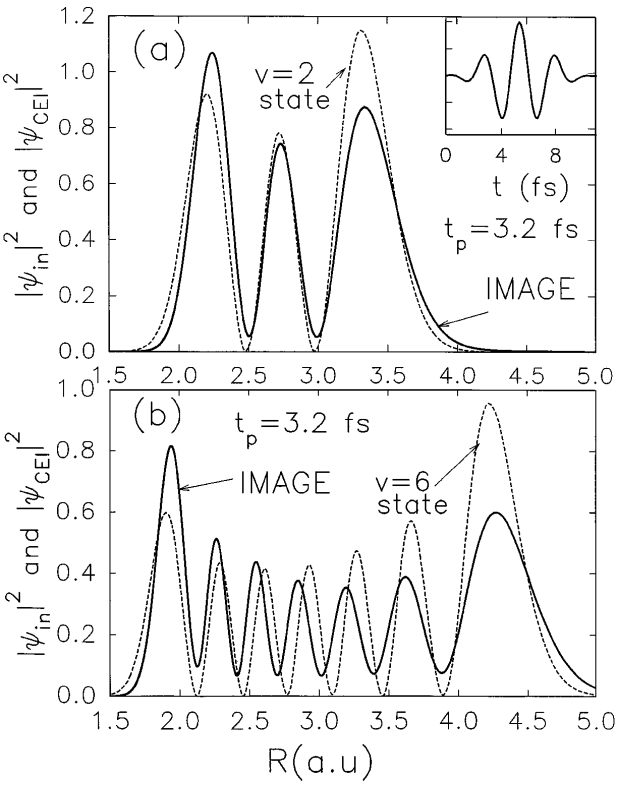

FIG. 3. $|\Psi_{\rm in}(R)|^2$ for the $v = 2$ (a) and the $v = 6$ (b) vibrational states plotted together with the simulated Coulomb explosion imaged $|\Psi_{\rm CEI}(R)|^2$. Note the significant offset of the imaged and initial wave function. The time dependent electric field for the 3.2 fs full width at half maximum laser pulse is shown in the inset.

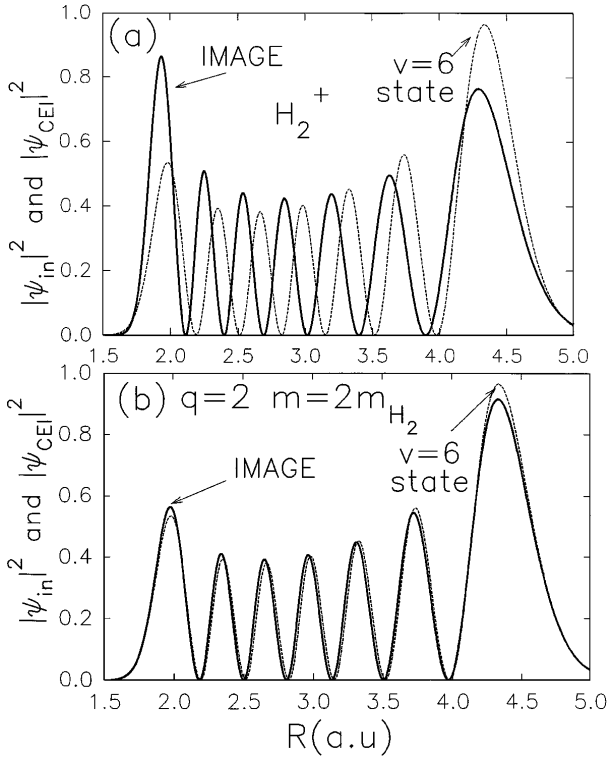

FIG. 4. (a) $|\Psi_{\rm in}(R)|^2$ and $|\Psi_{\rm CEI}(R)|^2$ obtained by an artificial Coulomb explosion where the ground state wave function is placed on the Coulomb repulsion curve. Note the similarity with Fig. 3(b). (b) When Coulomb explosion approximation is tested for higher mass and charge nuclei, the quality of reconstruction is greatly improved.

Figure 4(a) shows an initial $v = 6$ wave function calculated by propagating the initial wave packet $\Psi_{\rm in}(R)$ on the repulsive surface q^2/R. That is, we solved the time dependent Schrödinger equation for protons, without the laser field (and without the electron). The initial and imaged wave functions are almost identical to those shown in Fig. 3(b), indicating that the distortions seen in Fig. 3(b) are inherent in the classical reconstruction and unrelated to either ionization or the pulse rise time.

The relation of $\Psi_{\rm in}(R)$ to the energy distribution $S(E)$, for the case of quantum evolution on the repulsive surface with no laser field, is given by a Franck-Condon factor:

$$S(E) = |c(E)|^2 = \left| \int_0^\infty \varphi_c^*(E,R)\psi_{\rm in}(R)\, dR \right|^2 . \quad (4)$$

In the limit of a steeply repulsive curve and high masses the Coulomb wave $\varphi_c(E,R)$ under the integral in (4) can be replaced by the Dirac-δ function [15]

$$\varphi_c(E,R) = \frac{E}{q}\,\delta(E - q^2/R). \quad (5)$$

Inserting Eq. (5) into Eq. (4) yields the classical imaging prescription in Eq. (3). Classical imaging works best for well-localized Coulomb waves [on the scale of oscillations of $\psi_{\rm in}(R)$], otherwise quantum distortions in the image will occur. In Figs. 2 and 3 the first peaks of $|\Psi_{\rm CEI}(R)|^2$ are too high because the oscillations of the input wave and Coulomb wave overlap, whereas no overlap occurs for the last peak. The distortion caused by the classical Coulomb explosion imaging approximation will decrease for both higher charge states and larger ion masses. Figure 4(b) shows that these distortions have almost disappeared for $m = 2m_{\rm H_2}$, $q = 2$. (Note: Much of the difference between $|\Psi_{\rm in}(R)|^2$ and $|\Psi_{\rm CEI}(R)|^2$ is caused by neglecting the initial momentum associated with $\Psi_{\rm in}(R)$ in the reconstruction procedure. Using $|\Psi_{\rm CEI}(R)|^2$ to estimate the momentum distribution, some of the distortions can be corrected for H_2^+).

Although we have concentrated on H_2^+, where simulations can be rigorously performed, optical Coulomb explosion imaging will be widely useful. The agreement between $|\Psi_{\rm in}(R)|^2$ and $|\Psi_{\rm CEI}(R)|^2$ in Fig. 4(b) indicates that larger mass diatomic molecules with Coulomb-like dissociative states (e.g., D_2^+, Na_2^{2+}, Ca_2^{4+}) can be imaged. For nonclosed shell ions, bonding electrons play a role [3], introducing an additional error in the image at small R. However, ionizing to higher charge states can always be used to minimize this error [3].

Looking to the future, our work is most important because of timed Coulomb explosion imaging. By showing

that we can accurately image wave functions (structure), we imply that we can follow structural evolution (such as isomerization, and dissociation). In timed Coulomb explosion imaging [1,2] the probe pulse in a femtosecond pump-probe experiment triggers a Coulomb explosion. Pump-probe techniques introduce dynamics and the image is a snapshot of a changing molecular structure. In fact, our results show that nuclear motion can be followed. The difference between the position of the peaks in $|\Psi_{\mathrm{CEI}}(R)|^2$ seen in Fig. 2 (pulse duration 4.5 fs) and Fig. 3 (pulse duration 3.2 fs) is caused by movement of the nuclei (wave packet) on the laser modified $H_2{}^+$ potential surfaces [9,14]. (The cause of the movement is confirmed by modeling $H_2{}^+$ dissociation in the intense field using the strongly coupled σ_g and σ_u levels in a two-surface model.)

In conclusion, since imaging chemical reactions is one of the major challenges of modern science, the ability to freeze virtually all nuclear motion on the time scale for ionization is an important new tool. Both the laser [7,13] and the ion imaging technology [16,17] are developed, making femtosecond Coulomb explosion imaging experiments accessible. At least two other methods (ultrafast x-ray [18] and electron beam [19] scattering) are currently being pursued for observing the changing 3-dimensional structure of a polyatomic molecule. By using laser pulses to directly image molecules instead of producing electrons or x rays which are used in turn for imaging, Coulomb explosion imaging retains the ability to observe the fastest nuclear motion, even proton dynamics.

[1] H. Stapelfeldt, E. Constant, and P. B. Corkum, Phys. Rev. Lett. **74**, 3780 (1995).
[2] C. Ellert *et al.,* Philos. Trans. R. Soc. London A **356**, 329 (1998).
[3] P. B. Corkum, M. Yu. Ivanov, and J. S. Wright, Annu. Rev. Phys. Chem. **48**, 387 (1997).
[4] E. Aubanel and A. D. Bandrauk, Chem. Phys. Lett. **197**, 419 (1992).
[5] S. Chelkowski *et al.,* Phys. Rev. A **52**, 2977 (1995); K. C. Kulander, F. H. Mies, and K. J. Schafer, Phys. Rev. A **53**, 2562 (1996); S. Chelkowski, C. Foisy, and A. D. Bandrauk, Phys. Rev. A **57**, 1176 (1998).
[6] Z. Vager, R. Naaman, and E. P. Kanter, Science **244**, 426 (1989); D. Zajfman and Z. Amitay, Phys. Rev. A **52**, 839 (1995); J. Levin *et al.,* Phys. Rev. Lett. **81**, 3347 (1998).
[7] M. Nisoli *et al.,* Opt. Lett. **22**, 522 (1997).
[8] D. T. Strickland *et al.,* Phys. Rev. Lett. **68**, 2755 (1992).
[9] P. Dietrich and P. B. Corkum, J. Chem. Phys. **97**, 3187 (1992).
[10] A. Talebpour, S. Larochelle, and S. L. Chin, J. Phys. B **31**, L1 (1998).
[11] P. B. Corkum, Phys. Rev. Lett. **71**, 1994 (1993).
[12] *Handbook of Mathematical Functions,* edited by M. Abramovitz and I. R. Stegen (Dover Publications, Inc., New York, 1972); (We used $G_0 + iF_0$, given by Eq. 14.6.11. This solution satisfies the radial Schrödinger equation [defined by Eq. 14.1.1], which for $L = 0$, coincides with our 1D Schrödinger equation.)
[13] Ch. Spielmann *et al.,* Science **278**, 661 (1997).
[14] A. Conjusteau, A. D. Bandrauk, and P. B. Corkum, J. Chem. Phys. **106**, 9095 (1997).
[15] J. P. Laplante and A. D. Bandrauk, Chem. Phys. Lett. **42**, 184 (1976).
[16] A. J. R. Heck and D. W. Chandler, Annu. Rev. Phys. Chem. **46**, 335 (1995).
[17] K. A. Hanold, M. C. Ganer, and R. E. Continetti, Phys. Rev. Lett. **77**, 3335 (1996).
[18] C. Rischel *et al.,* Nature (London) **390**, 490 (1997).
[19] J. C. Williamson *et al.,* Nature (London) **386**, 159 (1997).